Manufacture of Optical Waveguide Preforms by Modified Chemical Vapor Deposition

Manufacture of optical waveguide preforms by modified chemical vapor deposition (MCVD) is theoretically investigated. For the first time, a model accounting for the concurrent heat transfer, chemical kinetics, and silica aerosol dynamics during lightguide preform fabrication by MCVD is presented. Silica particles are formed by high-temperature oxidation of $SiCl_4$, grow by coagulation, and deposit to the preform walls by thermophoresis and Brownian diffusion. Assuming first-order $SiCl_4$ oxidation and approximating the aerosol size distribution by a log normal function throughout the process, five partial differential equations describe this process. The emphasis of this study is on the achievement of high process yield (deposition efficiency of MCVD).

Process conditions for operation in the particle transport-limited and reaction-limited regimes are quantitatively identified. Operation in the former regime results in complete oxidation of the inlet $SiCl_4$ but only about half of the product SiO_2 particles deposit to the tube wall. Operation in the latter regime results in limited oxidation of inlet $SiCl_4$ (about 40%) but almost all product SiO_2 particles deposit to the tube wall. This study shows that high process yields and deposition rate can be achieved in lightguide preform manufacture by MCVD by combining operation in the reaction-limited regime with recycling of the exit gases from the preform tube.

Kyo-Seon Kim, Sotiris E. Pratsinis
Department of Chemical
and Nuclear Engineering
Center for Aerosol Processes
University of Cincinnati
Cincinnati, OH 45221

Introduction

Optical waveguides are threadlike structures of 10–100 μm dia. that are used for transmission of electromagnetic signals over long distances (Kao, 1982). To satisfy stringent purity requirements for low transmission losses, optical waveguides are drawn from glassy preform rods of 2–3 cm dia. that are made by vapor and particle deposition processes (Sarkar, 1985). The manufacture of the preform rod is one of the most important steps in the production of optical waveguides since the transmission properties (radial distribution of the refractive index) of the product optical waveguide are identical to those of the preform (Partus and Saifi, 1980). More than half of the worldwide production of optical waveguide preforms is made by modified chemical vapor deposition (MCVD). According to this process, O_2, $SiCl_4$, and dopant vapors ($GeCl_4$, $POCl_3$, BCl_3) flow through a rotating fused silica tube that is externally heated by a slow, axially traversing, oxyhydrogen torch. Inside the tube, the halides are oxidized forming oxide particles that either deposit to the tube walls or exit the tube with the process gases. Aside from oxidizing the reactant halides, the heat from the traversing torch also fuses the deposited particles and thus a glassy layer is formed in the interior of the substrate tube. The fabrication of the preform rod is completed when the successively deposited particle layers (30–100) almost fill the substrate tube (Nagel et al., 1982).

MacChesney et al. (1974) invented the MCVD process for fabrication of optical waveguide preforms. Simpkins et al. (1979) carried out a series of experiments proving that thermophoresis is the dominant mass transfer mechanism in MCVD. Walker et al. (1979) theoretically studied submicron, monosize particle transport by thermophoresis in laminar tube flows and developed analytical and numerical solutions for the particle deposition efficiency (fraction of inlet particles deposited to the tube walls). They proposed that the total deposition efficiency depends on the maximum and minimum temperatures of the substrate tube, $T_{min}/(T_{max} - T_{min})$, and the product of thermo-

Correspondence concerning this paper should be addressed to S. E. Pratsinis.

phoretic coefficient and Prandtl number (KPr). Walker et al. (1980) extended this model to the description of the MCVD process by neglecting the oxidation reaction and aerosol dynamics inside the preform tube. They developed a quantitative criterion for the length of the preform deposition zone and successfully predicted the process yield (deposition efficiency) of industrial MCVD units. Weinberg (1982 and 1983) developed similar models for MCVD and indicated that perfect process yields can be achieved provided that particle formation is confined near the substrate tube or the temperature gradient between gas stream and tube wall is maintained along the tube. Morse and Cipolla (1984) and Morse et al. (1985, 1986) also reported that the deposition efficiency in the MCVD process can be substantially improved by increasing and maintaining the temperature gradient inside the preform tube by axial laser heating of the process gases.

Despite the industrial importance of MCVD, the production of optical waveguide preforms still relies heavily on empirical measures and observations. Currently the process yield is about 50% with respect to SiO_2 and it is much lower for costly dopants. No current literature models for MCVD account for the precursor vapor chemical kinetics and oxide aerosol dynamics. As a result, these models cannot quantitatively relate process variables (inlet halide vapor concentration, torch temperature, total gas flow rate) to process characteristics (process efficiency, deposited layer composition and, subsequently, preform refractive index profile).

This paper presents a model for MCVD accounting for the concurrent vapor oxidation kinetics and product aerosol dynamics (coagulation, diffusion, thermophoresis) through the coupled energy and vapor mass balances and the general dynamic equation for aerosols. The model is validated by comparing its predictions with known solutions at various limiting cases. Detailed profiles for gas temperature, $SiCl_4$ concentration, and SiO_2 particle concentration and average size along the preform axis are presented assuming first-order $SiCl_4$ oxidation rate (Powers, 1978) and approximating the SiO_2 aerosol size distribution by a log normal function throughout the MCVD process (Pratsinis, 1988). The focus of this study is, however, on the prediction of the process yield. Thus, simulation conditions similar to those encountered in industrial MCVD units are selected and process conditions and designs resulting in highly efficient production of lightguide preforms are investigated.

Theory

Nagel et al. (1982) presented a detailed picture of the commercial MCVD process. Here, a quantitative description of a simplified version of this process (deposition of a single species in a stationary, uniformly heated glass tube) is used to elucidate the fundamental physicochemical phenomena taking place during MCVD, Figure 1. Reactant gases ($SiCl_4$ vapor in excess O_2) enter the externally heated region (reaction zone) of the substrate (preform) tube in fully developed, incompressible laminar flow. There, the gas temperature is raised high enough that $SiCl_4$ is oxidized, resulting in SiO_2 and Cl_2. Silica particles are instantaneously formed and grow by Brownian coagulation. These particles flow out of the reaction zone into the low-temperature section of the tube (deposition zone). There, some particles deposit to the tube walls by Brownian diffusion and thermophoresis while the rest exit the tube by convection. This

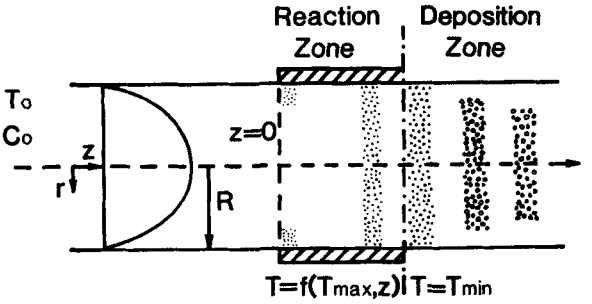

Figure 1. Simplified MCVD process.
$SiCl_4$ and O_2 enter the substrate tube where they are heated and react, forming SiO_2 particles (reaction zone) that deposit to the cool tube walls (deposition zone)

process is described by the energy and precursor vapor balances and the general dynamic equation for the silica aerosol.

Assuming negligible axial heat diffusion ($Pe_h \gg 1$), negligible free convection (Kays and Perkins, 1985; Figure 29), and first-order $SiCl_4$ oxidation kinetics (Powers, 1978; French et al., 1978; Kleinert et al., 1980), the energy balance inside the preform tube is:

$$2U\left[1-\left(\frac{r}{R}\right)^2\right]\frac{\partial T}{\partial z}=\frac{\alpha}{r}\frac{\partial}{\partial r}\left(r\frac{\partial T}{\partial r}\right)+\frac{\Delta H k_0}{\rho c_p}\exp\left(\frac{-E}{R_G T}\right)C \quad (1)$$

The first term on the righthand side (RHS) accounts for radial heat transfer by conduction. The second RHS term in Eq. 1 accounts for the released heat from the exothermic oxidation of $SiCl_4$. The gas temperature at the tube inlet ($z = 0$) is T_0 and the boundary condition at the tube centerline ($r = 0$) is $\partial T/\partial r = 0$. The temperature profile at the tube wall is a function of axial distance (Morse et al., 1985). Thus, in the reaction zone ($0 \le z < L_2$):

$$T = T_0 + (T_{max} - T_0)(z/L_1)^2 \quad \text{for } 0 \le z < L_1 \quad (2)$$

and

$$T = T_{max} - (T_{max} - T_{min})(z - L_1)/(L_2 - L_1) \quad \text{for } L_1 \le z < L_2 \quad (3)$$

while in the deposition zone ($z \ge L_2$):

$$T = T_{min} \quad (4)$$

Assuming negligible axial $SiCl_4$ vapor diffusion compared to convection ($Pe_m \gg 1$), the $SiCl_4$ vapor mass balance inside the preform tube is:

$$2U\left[1-\left(\frac{r}{R}\right)^2\right]\frac{\partial C}{\partial z}=\frac{\mathcal{D}}{r}\frac{\partial}{\partial r}\left(r\frac{\partial C}{\partial r}\right)-k_0\exp\left(\frac{-E}{R_G T}\right)C \quad (5)$$

The first RHS term in Eq. 5 accounts for radial diffusion of $SiCl_4$ vapor and the second term accounts for consumption of $SiCl_4$ by oxidation. At $z = 0$, the $SiCl_4$ concentration is C_0 and the boundary conditions of Eq. 5 are $\partial C/\partial r = 0$ at $r = 0$ and $r = R$, assuming no flux of $SiCl_4$ to the preform walls (neglecting chemical vapor deposition).

For silica particles undergoing diffusion, thermophoresis, and

coagulation in the size range v, $v + dv$, the general dynamic equation is (Friedlander, 1977):

$$2U\left[1 - \left(\frac{r}{R}\right)^2\right]\frac{\partial n}{\partial z} = \frac{1}{r}\frac{\partial}{\partial r}\left[r\frac{\partial(Dn)}{\partial r}\right] + \frac{K\nu}{r}\frac{\partial}{\partial r}\left(nr\frac{\partial \ln T}{\partial r}\right) + \frac{1}{2}\int_0^v \beta(v, v - \bar{v})n(v)n(v - \bar{v})\,d\bar{v} - \int_0^\infty \beta(v, \bar{v})n(v)n(\bar{v})\,d\bar{v} + S\delta(v - v_1) \quad (6)$$

The first RHS term in Eq. 6 accounts for particle losses by Brownian diffusion. The particle diffusivity is related to particle size (Friedlander, 1977):

$$D = \frac{k_B T}{3\pi\mu}\left\{\frac{1}{d_p} + \frac{2\lambda}{d_p^2}\left[A_1 + A_2 \exp\left(\frac{-A_3 d_p}{\lambda}\right)\right]\right\} \quad (7)$$

where $A_1 = 1.257$, $A_2 = 0.4$, and $A_3 = 0.55$. The second RHS term in Eq. 6 accounts for particle losses by thermophoresis (Walker et al., 1979). In principle, the thermophoretic coefficient is related to particle size by a correlation over the entire particle size spectrum (Talbot et al., 1980). However, for silica particles less than 1 μm dia., K is constant and equal to 0.55 (Mehrotra and Alam, 1986). The third and fourth RHS terms in Eq. 6 account for particle gain and loss by Brownian coagulation. For coagulation in the free molecule size regime, the collision frequency function is (Friedlander, 1977):

$$\beta_{FM} = \left(\frac{3}{4\pi}\right)^{1/6}\left(\frac{6k_B T}{\rho_p}\right)^{1/2}\left(\frac{1}{v} + \frac{1}{\bar{v}}\right)^{1/2}(v^{1/3} + \bar{v}^{1/3})^2 \quad (8)$$

while for coagulation in the continuum-slip regime, the coefficient is (Lee and Chen, 1984):

$$\beta_C = \frac{2k_B T}{3\mu}\left[\frac{B(v)}{v^{1/3}} + \frac{B(\bar{v})}{\bar{v}^{1/3}}\right](v^{1/3} + \bar{v}^{1/3}) \quad (9)$$

where $B(v)$ is the Cunningham correction factor, $B = 1 + 2A_1\lambda/d_p$. The last RHS term in Eq. 6 accounts for the formation of new particles by chemical reaction. Silica particles are instantaneously formed since nucleation of silica by oxidation of $SiCl_4$ cannot be distinguished from chemical reaction (Ulrich, 1971). Thus, the size of the newly formed particles is equal to the equivalent molecular diameter of SiO_2 ($d_p^* = 4.35$ Å). The rate of particle formation is equal to the oxidation rate of $SiCl_4$ (Powers, 1978):

$$S = N_{av}k_0 \exp(-E/R_G T)C \quad (10)$$

In principle, one needs to write a number of general dynamic equations like Eq. 6 along with the auxiliary Eqs. 7–10 at each streamline to cover the silica aerosol dynamics over the entire particle size spectrum. Although this approach can be followed using accurate numerical models from the literature (Tsang and Brock, 1984; Warren and Seinfeld, 1985), the computational efficiency of these models is uncertain for highly nonuniform-nonisothermal aerosol processes (Brock and Oates, 1987) such as the manufacture of optical waveguide preforms. An alternative approach is the description of the aerosol dynamics through the evolution of the moments, M_q, of the aerosol size distribution:

$$M_q = \int_0^\infty nv^q\,dv \quad (11)$$

The use of moments has the advantage of simplicity while providing the most important information about the process (Pratsinis et al., 1986). The evolution of the qth silica aerosol moment is obtained by substituting Eqs. 7–10 into Eq. 6, multiplying both sides of Eq. 6 by v^q, and integrating over all particle sizes. It is to be hoped that a few moment balance equations suffice to describe the silica aerosol dynamics. The major difficulties for this procedure lie, first, in the form of the functions describing the basic particulate processes (collision frequency function for free-molecule regime and particle diffusivity) and, second, in the closure of the moment model. The collision frequency function in the free-molecule regime can be brought to an integrable form by using the approximation (Lee and Chen, 1984):

$$(1/v + 1/\bar{v})^{1/2} = b(1/v^{1/2} + 1/\bar{v}^{1/2}) \quad (12)$$

where b is a function of the width of the aerosol size distribution. The particle diffusivity can be brought to an integrable form by following the procedure of Lee and Liu (1980) in Eq. 7:

$$D = \frac{k_B T}{3\pi\mu}\left(\frac{1}{d_p} + \frac{3.314\lambda}{d_p^2}\right) \quad (13)$$

This expression overpredicts D by 2–11% for $0.1 < Kn < 10$ and by less than 2% for all other Kn (Pratsinis and Kim, 1988). Using the above approximations for β_{FM} and D, moment equations can be written for any power of v.

A closed set of moment equations, however, cannot be achieved unless the shape of the aerosol size distribution is approximated by a specific function. For this purpose, a unimodal log normal function is used here since many experimental results indicate that aerosol size distributions are nearly log normal (Okuyama et al., 1986, Figure 5) or, more frequently, aerosols are measured and characterized using the parameters of a log normal function (Ingebrethsen et al., 1983, Table I). These parameters are the total particle concentration M_0, the geometric average particle volume $v_g = M_1^2/(M_0^3 M_2)^{1/2}$, and the geometric standard deviation σ, $[\ln^2\sigma = \ln(M_0 M_2/M_1^2)/9]$. Thus, the first three moments of the distribution are sufficient to describe the aerosol dynamics and the qth moment of the distribution can be written in terms of the above parameters as:

$$M_q = M_0 v_g^q \exp(4.5q^2 \ln^2\sigma) \quad (14)$$

Subsequently, the evolution of the zero aerosol moment (total particle concentration) is written as:

$$2U\left[1 - \left(\frac{r}{R}\right)^2\right]\frac{\partial M_0}{\partial z} = \frac{B_1}{r}\frac{\partial}{\partial r}\left[r\frac{\partial}{\partial r}(M_{-1/3} + B_2 M_{-2/3})\right] + \frac{K\nu}{r}\frac{\partial}{\partial r}\left(M_0 r\frac{\partial \ln T}{\partial r}\right) - \xi M_0^2 + k_0 N_{av}\exp\left(\frac{-E}{R_G T}\right)C \quad (15)$$

where the coagulation coefficient ξ is the harmonic average of

the coagulation coefficients in the continuum and free-molecule size regimes (Fuchs and Sutugin, 1971; Pratsinis, 1988):

$$\xi = \xi_{FM}\xi_C/(\xi_{FM} + \xi_C) \tag{16}$$

$$\xi_C = B_3\left\{1 + \exp(\ln^2\sigma) + \frac{B_4}{v_g^{1/3}}\exp\left(\frac{1}{2}\ln^2\sigma\right)[1 + \exp(2\ln^2\sigma)]\right\} \tag{17}$$

$$\xi_{FM} = B_5 b_0 v_g^{1/6}\left[\exp\left(\frac{25}{8}\ln^2\sigma\right) + 2\exp\left(\frac{5}{8}\ln^2\sigma\right) + \exp\left(\frac{1}{8}\ln^2\sigma\right)\right] \tag{18}$$

$$b_0 = 0.633 + 0.092\sigma^2 - 0.022\sigma^3 \tag{19}$$

The evolution of the first aerosol moment (total aerosol volume) is written as:

$$2U\left[1 - \left(\frac{r}{R}\right)^2\right]\frac{\partial M_1}{\partial z} = \frac{B_1}{r}\frac{\partial}{\partial r}\left[r\frac{\partial}{\partial r}(M_{2/3} + B_2 M_{1/3})\right] + \frac{K\nu}{r}\frac{\partial}{\partial r}\left(M_1 r\frac{\partial \ln T}{\partial r}\right) + k_0 N_{av} v_1 \exp\left(\frac{-E}{R_G T}\right)C \tag{20}$$

The evolution of the second aerosol moment is written as:

$$2U\left[1 - \left(\frac{r}{R}\right)^2\right]\frac{\partial M_2}{\partial z} = \frac{B_1}{r}\frac{\partial}{\partial r}\left[r\frac{\partial}{\partial r}(M_{5/3} + B_2 M_{4/3})\right] + \frac{K\nu}{r}\frac{\partial}{\partial r}\left(M_2 r\frac{\partial \ln T}{\partial r}\right) + 2\zeta M_1^2 + k_0 N_{av} v_1^2 \exp\left(\frac{-E}{R_G T}\right)C \tag{21}$$

where the coagulation coefficient for the second moment, ζ, is (Pratsinis, 1988):

$$\zeta = \zeta_{FM}\zeta_C/(\zeta_{FM} + \zeta_C) \tag{22}$$

$$\zeta_C = B_3\left\{1 + \exp(\ln^2\sigma) + \frac{B_4}{v_g^{1/3}}\exp\left(\frac{-1}{2}\ln^2\sigma\right)\cdot[1 + \exp(-21n^2\sigma)]\right\} \tag{23}$$

$$\zeta_{FM} = B_5 b_2 v_g^{1/6}\exp\left(\frac{3}{2}\ln^2\sigma\right)\left[\exp\left(\frac{25}{8}\ln^2\sigma\right) + 2\exp\left(\frac{5}{8}\ln^2\sigma\right) + \exp\left(\frac{1}{8}\ln^2\sigma\right)\right] \tag{24}$$

$$b_2 = 0.39 + 0.5\sigma - 0.214\sigma^2 + 0.029\sigma^3 \tag{25}$$

Assuming that the reactant gases are free of particles at the preform inlet, the initial conditions for the moments are:

$$\text{at } z = 0, \quad M_0 = M_1 = M_2 = 0 \tag{26}$$

Cylindrical symmetry dictates the boundary conditions at the tube centerline:

$$\text{at } r = 0, \quad \frac{\partial M_0}{\partial r} = \frac{\partial M_1}{\partial r} = \frac{\partial M_2}{\partial r} = 0 \tag{27}$$

Assuming that every particle arriving at the wall sticks there (no resuspension of particles), the wall boundary conditions are:

$$\text{at } r = R, \quad M_0 = M_1 = M_2 = 0 \tag{28}$$

Eqs. 1–5, 14–28 constitute a system of coupled algebraic and partial differential equations (PDE) that describes silica formation and deposition inside the preform tube. Using an explicit finite-difference scheme (Ferziger, 1981) at P radial points across the preform tube, the five PDE's are converted to $5 \times P$ ordinary differential equations (ODE) (Kim, 1988). The ODE's are solved by an efficient algorithm for stiff equations (here by DGEAR, IMSL, 1980).

Once the profiles of temperature, $SiCl_4$ concentration, and silica aerosol moments are calculated along the preform tube axis, the MCVD process parameters (efficiency, reactant conversion, silica volume average diameter, and polydispersity) are calculated from the mixing cup averages of the moments. The reactant conversion, E_R, is the fraction of the inlet reactant gas ($SiCl_4$) that was oxidized ($E_R = 1 - C_m/C_0$). The process yield (deposition efficiency), E_D, is the equivalent fraction of inlet reactant gas (here, $SiCl_4$) that was deposited onto the substrate tube ($E_D = E_R - M_{1m}/C_0 N_{av} v_1$). The volume average diameter is $d_p = (6M_1/\pi M_0)^{1/3}$, and the aerosol polydispersity index, $W = (M_{2/3}M_0/M_{1/3}^2 - 1)^{1/2}$, is a measure of the spread of the silica particle size distribution (Pratsinis et al., 1986).

Results and Discussion

The accuracy of the numerical scheme was investigated by comparing the solution of the heat equation in the absence of the heat of reaction and fixed wall temperature with the series solution of Carslaw and Jaeger (1980). Excellent agreement was obtained between the two techniques. Simultaneous solution of Eqs. 1 and 6 in the absence of chemical reaction, particle diffusion, and coagulation describes particle transport to tube walls by thermophoresis in nonisothermal laminar tube flow. Figure 2 shows that good agreement was obtained between the computed asymptotic deposition efficiency by this model with that computed by trajectory calculations (Walker et al., 1979) for various KPr and T^* (Pratsinis and Kim, 1988). The numerical scheme has also been found in excellent agreement with literature results when only particle diffusion (Hinds, 1982, Figure 7.9) or only coagulation (Lee, 1983; Lee et al., 1984) is operating (Pratsinis and Kim, 1988).

Table 1 lists the employed process conditions for simulation of MCVD. The inner diameter of the preform tube, inlet $SiCl_4$ concentration, gas flow rate, and minimum, maximum, and inlet temperatures are typical for industrial MCVD processes (Walker et al., 1980; Simpkins et al., 1979). All transport properties of the carrier gas (O_2) and the constants, B_i, have been estimated at the average process temperature, T_e, to simplify the computations (Walker et al., 1980). The $SiCl_4$ diffusivity was estimated from the Chapman-Enskog equation (Bird et al., 1960). The employed low particle volume fractions, Reynolds, Grashof, and Peclet numbers are in agreement with our assump-

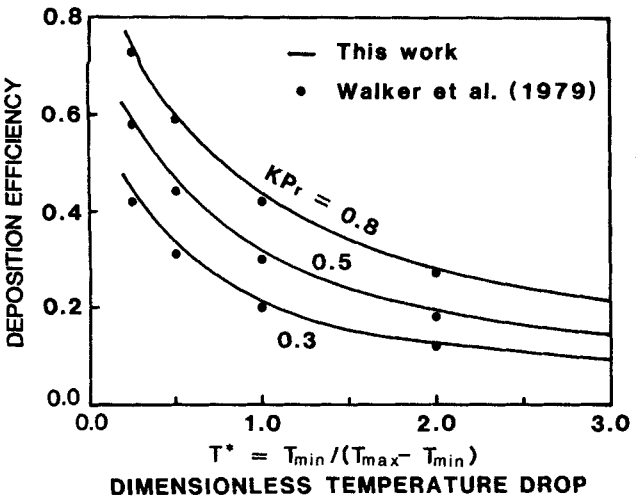

Figure 2. Deposition efficiency of particles in laminar tube flow by thermophoresis as a function of T^* and KPr.

tions for laminar flow, negligible natural convection, and negligible axial heat and mass diffusion compared to convection.

Reaction of $SiCl_4$ and deposition of SiO_2 at the walls of the reaction zone by chemical vapor deposition are neglected since silica deposits have not been observed at the torch area of the preform during MCVD (Simpkins et al., 1979). In this model, it is assumed that all particles coalesce after colliding. This assumption does not affect the silica deposition rate, which is controlled by thermophoresis, a particle transport mechanism independent of size for submicron particles. This assumption may, however, affect, the coagulation rate of silica and subsequently the predicted particle concentration, average size, and polydispersity since silica particles are produced in the form of irregular aggregates (Ulrich and Subramanian, 1977). In modeling coagulation of irregular particles, the collision rate of spherical particles is usually scaled by a shape (or bulkiness) factor. For example, Ulrich and Riehl (1982) arbitrarily used 1.2 as a shape factor for SiO_2 coagulation during oxidation of $SiCl_4$ in laminar flames. Here, the effects of particle shape and van der Waals forces on silica coagulation are not included in these simulations. Finally, in this model the silica aerosol dynamics are described efficiently by approximating the aerosol size distribution by a log normal function throughout the MCVD process. It should be noted, however, that a unimodal log normal function may not always give an accurate description of the detailed particle size distribution, especially during new particle (here, SiO_2 monomer) formation. Nevertheless, this function always gives a consistent and fairly accurate description of the effects of various physicochemical phenomena (nucleation, condensation, coagulation, and diffusion) on the key aerosol characteristics such as particle concentration, volume average diameter (Brock and Oates, 1987), polydispersity (Pratsinis, 1988), and penetration/deposition efficiency (Lee and Gieseke, 1980).

Figures 3–6 show radial profiles of the process variables in the reaction (solid lines) and deposition (broken lines) zones of the preform ($P = 10$). Figure 3 indicates that the temperature profile is parabolic (concave in heating [$z/R \leq 20$] and convex in cooling [$z/R > 20$]) throughout the process at $T_{max} = 1{,}500$°C. Thus, the temperature inside the preform tube is determined primarily by radial heat conduction while the released heat from the exothermic oxidation of $SiCl_4$ is important only in a small section of the reaction zone of the preform. Specifically, for the values of ΔH, ρ, c_p, and C_0 of Table 1, the released heat from the oxidation reaction corresponds to a 172°C rise of the carrier gas temperature at adiabatic conditions. The MCVD process, however, is not an adiabatic one. Thus, the released heat from the exothermic reaction increases the gas temperature, retarding additional radial heat transfer from the preform tube. When the

Table 1. Simulation Conditions for the MCVD Process

C_0	1.0×10^{-6} mol/cm^3	
L_1	20 cm	
L_2	22 cm	
Q	1 or 5 L/min	
R	1 cm	
T_0	800°C	
T_{max}	1,700 or 1,500°C	
T_{min}	180°C	
ρ_p	2.32 g/cm^3	
ΔH	251 kJ/mol	
k_0	1.7×10^{14} s^{-1}	
E	402 kJ/mol	
	$T_e = 940$°C ($T_{max} = 1{,}700$°C)	$T_e = 840$°C ($T_{max} = 1{,}500$°C)
$\mathcal{D}$	0.83 cm^2/s	0.73 cm^2/s
μ	5.4×10^{-4} g/cm · s	5.1×10^{-4} g/cm · s
α	2.36 cm^2/s	2.04 cm^2/s
λ	3.76×10^{-5} cm	3.40×10^{-5} cm
ρ	3.22×10^{-4} g/cm^3	3.50×10^{-4} g/cm^3
c_p	1.09 J/g · K	1.07 J/g · K
Pe_h	18 (Q = 1 L/min)	19 (Q = 1 L/min)
Pe_m	52	55
Gr	3,477	4,368
Re	26	27

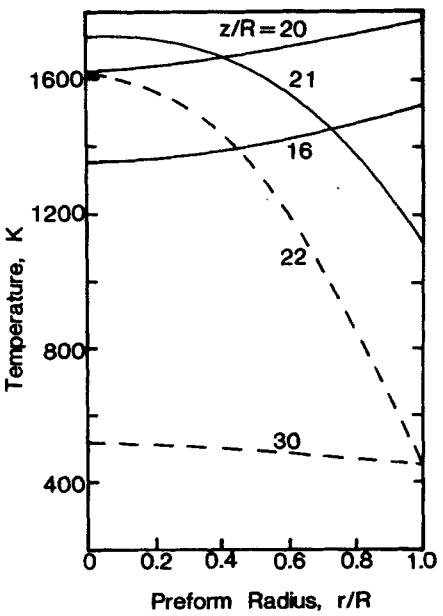

Figure 3. Temperature profiles inside preform tube.
—— Reaction zone; ---- deposition zone

heat of the oxidation is not accounted for ($\Delta H = 0$), the maximum centerline gas temperature is 122°C lower than that obtained with $\Delta H = 251$ kJ/mol at carrier gas flow rate $Q = 1$ L/min. The evolution of the dimensionless $SiCl_4$ concentration profile along the preform axis is shown in Figure 4. For $z/R \leq 16$, the gas temperature is not high enough for significant $SiCl_4$ oxidation to take place across the preform tube. Further downstream ($16 < z/R \leq 20$), the gas stream temperature is raised substantially and the $SiCl_4$ is almost completely oxidized at the exit of the reaction zone.

Figure 5 shows the evolution of the radial profile of total silica particle concentration along the preform axis. Early in the reaction zone ($z/R \leq 16$), some silica particles are formed close to the preform walls. For $16 < z/R \leq 20$, the particle concentration is determined by coagulation and chemical reaction. Thermophoresis and coagulation reduce particle concentration when the preform wall temperature is lower than that of the gas stream ($z/R > 20$). For the above conditions the particle concentration is determined by chemical reaction, coagulation, and thermophoresis while particle diffusion to the preform walls is not important. Radial diffusion of $SiCl_4$, however, is important. Figure 6 shows the dimensionless particle volume concentration profiles along the preform axis. At the beginning of the reaction zone, the particle volume increases near the tube wall where the reaction is fairly fast. As $SiCl_4$ is oxidized first near the preform wall, the local $SiCl_4$ concentration is depleted, and $SiCl_4$ diffuses from the centerline toward the region near the wall where it reacts forming SiO_2 particles. As a result, further downstream ($16 < z/R \leq 20$) more SiO_2 is present adjacent to the preform wall ($r/R > 0.7$) than the SiO_2 that corresponds to the inlet $SiCl_4$ ($M_1/C_0N_{av}v_1 = 1$ stoichiometrically for complete reaction). At the end of the reaction zone ($z/R = 20$), silica particles have accumulated near the preform wall (sharp peak at $0.7 < r/R < 1$) by the combined effects of $SiCl_4$ diffusion and oxidation. These particles, however, do not deposit to the wall because of the low particle diffusivity ($<10^{-5}$ cm^2/s) and the unfavorable temperature gradient. When the particle-laden stream is cooled ($z/R > 20$), these particles rapidly deposit to the preform walls by thermophoresis and the dimensionless particle volume decreases. Further downstream ($z/R \geq 30$), the silica volume concentration reaches its asymptotic profile across the preform tube. For these conditions, about 60% of the inlet $SiCl_4$ was deposited as SiO_2 onto the preform tube.

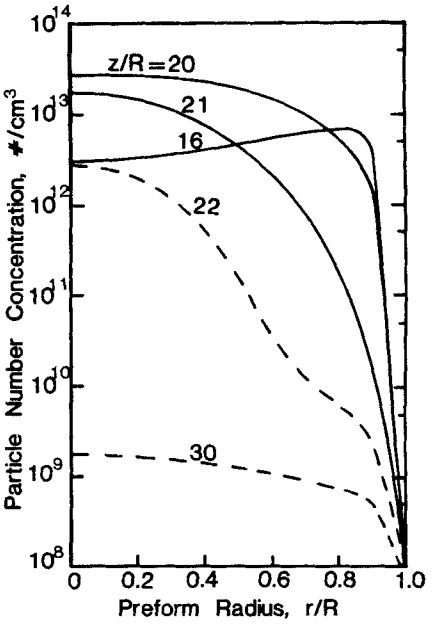

Figure 5. SiO_2 particle concentration profiles inside preform tube.

—— Reaction zone; ---- deposition zone

Walker et al. (1980) identified qualitatively two distinct operating regimes during MCVD: the particle transport-limited regime in which the deposition efficiency is limited by particle transport to preform walls, and the reaction-limited regime in which the deposition efficiency is limited by the extent of chemical reaction across the preform tube. They reported that in industrial units the latter regime is encountered at high gas flow rates (4–5 L/min). The present model can be used to determine quantitatively the process conditions under which particle transport-limited or reaction-limited operation takes place. Figure 7 shows the deposition efficiency (broken line) and the $SiCl_4$ con-

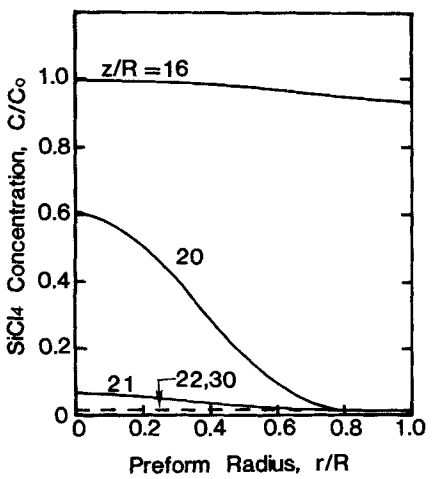

Figure 4. Dimensionless $SiCl_4$ concentration profiles inside preform tube.

—— Reaction zone; ---- deposition zone

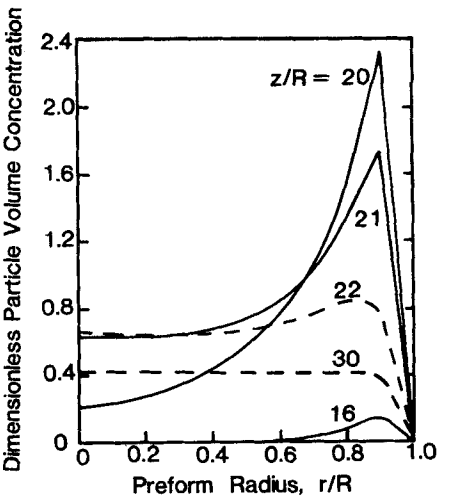

Figure 6. Dimensionless particle volume profiles inside preform tube.

—— Reaction zone; ---- deposition zone

version (solid line) along the preform axis for two gas flow rates, 1 and 5 L/min, and two maximum preform wall temperatures, 1,500 and 1,700°C. With T_{max} = 1,500°C, it is seen that at low gas flow rate (1 L/min) practically all inlet $SiCl_4$ is oxidized (98%) but only about 58% of the product SiO_2 is deposited, Figure 7a. This corresponds to operation in the particle transport-limited regime. At high gas flow rate, about 10% of the inlet $SiCl_4$ is oxidized and almost all product SiO_2 is formed only close to the tube wall and deposits there easily by thermophoresis while the process gases exit almost free of particles. Similar results are obtained when high torch temperatures, T_{max} = 1,700°C, are employed such as those used in industrial MCVD processes, Figure 7b. It should be noted, however, that typical flow conditions used in current industrial production of light-guide preforms are >5 L/min with $T_{max} \simeq$ 1,900°C. Most previously published temperature measurements were low by some 200°C because of the use of optical pyrometers that used a wavelength at which the glass was partially transparent (K. L. Walker, personal communication, 1988). Although $SiCl_4$ is fully converted at low flow rates, only 60% of the product SiO_2 deposits to the substrate tube. Of course, at the latter temperature higher $SiCl_4$ conversion rate and higher SiO_2 deposition efficiency are obtained than with T_{max} = 1,500°C. Operation of MCVD units at high gas flow rate clearly corresponds to operation in the reaction-limited regime. When the exothermicity of the oxidation reaction is not accounted for (ΔH = 0) in reaction-limited MCVD operation, the process yield (deposition efficiency) is lower by 10–20% depending on gas flow rate and torch temperature.

Although fully documented experimental data of MCVD are not available in the literature for a detailed comparison with this theory, the above predictions for the deposition efficiencies are in agreement with the reported deposition efficiencies of industrial MCVD units, 50 to 65% (Walker et al., 1980). The results

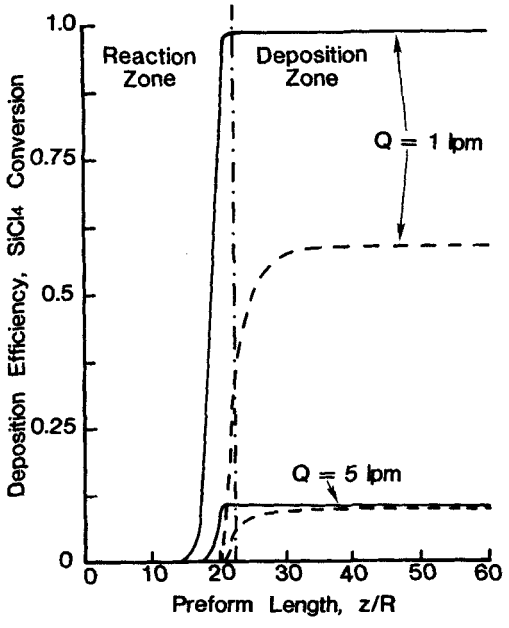

Figure 7a. Reaction extent (—) and deposition efficiency (----) along preform axis, T_{max} = 1,500°C.

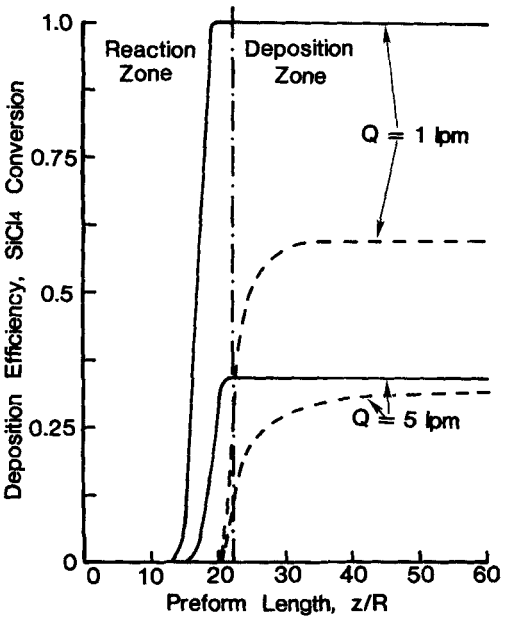

Figure 7b. Reaction extent (—) and deposition efficiency (----) along preform axis, T_{max} = 1,700°C.

of Figure 7 are in good agreement with the work of Walker et al. (1980) for the conditions (here gas flow rates) that separate MCVD operation in the particle transport-limited and reaction-limited regimes.

The results of Figure 7 can be used for the design and operation of highly efficient MCVD units. This can be accomplished by selecting the process conditions for operation in the reaction-limited regime and recycling the gases that exit the preform. Specifically for T_{max} = 1,700°C, Q = 5 L/min, and a recycle to fresh feed ratio 4:1, the overall deposition efficiency is above 70% while the single pass efficiency is 32%. Although this calculation is for a single (and inexpensive) species ($SiCl_4/SiO_2$) MCVD, this process yield is better than the current industrial yields for silica (50–65%). Operation at the above conditions reduces the preform fabrication time by more than 60% over that with operation in the particle transport-limited regime (Q = 1 L/min) without recycle. When the effluent gases are separated and recycled, the process yield can be close to 100%. This can be an economic incentive, especially for costly dopants such as $GeCl_4$ (Bohrer et al., 1985).

The proposed model for MCVD predicts the concentration, average diameter, and polydispersity of the newly formed particles along the axis of the preform. Figure 8 shows the mixing cup average particle concentration along the preform axis at two process gas flow rates with T_{max} = 1,700°C. The particle concentration increases inside the reaction zone as long as new particles are formed by chemical reaction. In the reaction zone, the particle concentration obtained at 1 L/min is higher than that obtained at 5 L/min since chemical reaction and subsequently particle formation take place for a longer time inside the preform. When the reaction ceases (by $SiCl_4$ exhaustion with Q = 1 L/min or by exiting the high temperature zone with Q = 5 L/min), coagulation rapidly reduces the particle concentration. In the deposition zone, lower particle concentrations are obtained

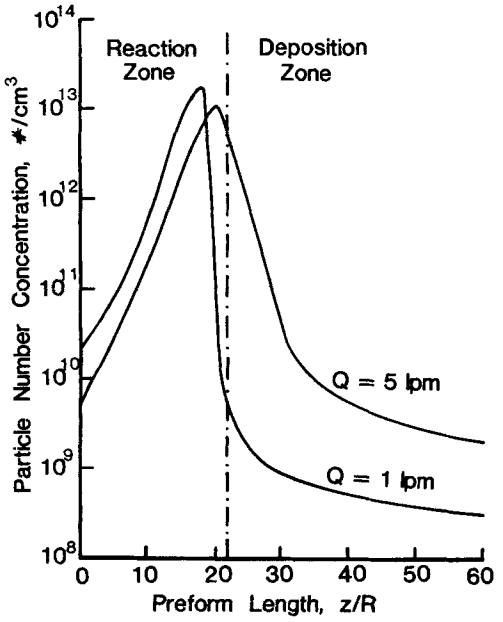

Figure 8. Mixing cup average particle concentration along preform axis, T_{max} = 1,700°C.

at low than at high flow rates since particle coagulation and deposition operate for longer time. Figure 9 shows that larger particles are formed at low rather than at high gas flow rates since SiO_2 coagulation takes place much longer, and also high $SiCl_4$ conversion (100 vs. 34%) is achieved and more SiO_2 remains in the gas phase (40 vs. 2% of the corresponding inlet $SiCl_4$) during preform fabrication at low gas flow rates (T_{max} = 1,700°C). Figure 10 shows that the polydispersity index of silica increases as new particles are generated across and along the reaction zone of the preform. Downstream in the deposition zone, the polydispersity index decreases by coagulation and reaches an asymptotic value, $W = 0.283$, corresponding to the asymptotic geometric standard deviation for coagulation in the continuum regime ($\sigma = 1.32$; Lee, 1983) at each streamline [$W = (\exp(\ln^2\sigma) - 1)^{1/2}$]. Lee observed that the asymptotic distribution is in reasonably good agreement with the self-preserving distribution (Friedlander and Wang, 1966). It should be noted, however, that the asymptotic W of Figure 10 is different

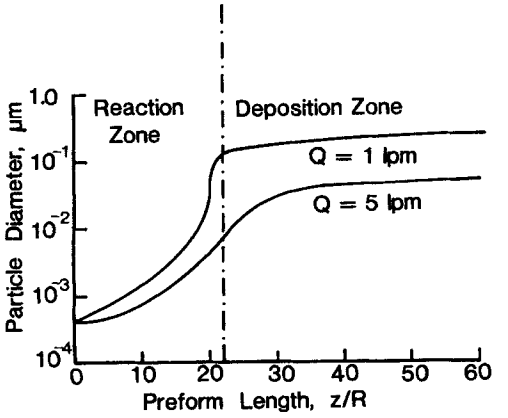

Figure 9. Mixing cup average particle diameter along preform axis, T_{max} = 1,700°C.

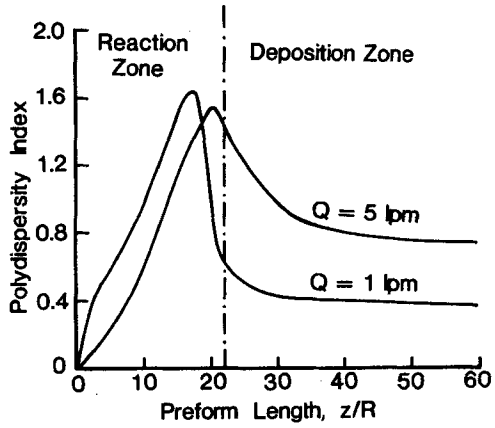

Figure 10. Polydispersity index of SiO_2 particles along preform axis, T_{max} = 1,700°C.

from 0.283 since the evolution of the mixing cup average W is shown along the preform axis. More polydisperse silica particles exit the preform tube at high than at low gas flow rates since strong radial differences of $SiCl_4$ conversion and thus SiO_2 particle sizes exist across the tube at the former gas flow rates. Note that, at high gas flow rates, two-thirds of the inlet $SiCl_4$ are not oxidized with T_{max} = 1,700°C. Knowledge of the particle size and polydispersity is important for understanding dopant incorporation and deposition during multicomponent MCVD of lightguide preforms (Wood et al., 1987). The current model can be extended to describe the more fascinating and industrially more important multicomponent MCVD.

Conclusions

A model accounting for the concurrent single-species oxidation kinetics and aerosol dynamics during lightguide preform manufacture by MCVD was developed. The performance of the model was validated by comparing its predictions with known solutions at certain limiting cases. This model unravels the importance of various physicochemical phenomena taking place during MCVD and relates process variables (vapor concentration, flow rate, torch temperature) to the MCVD process yield (deposition efficiency) and the characteristics (concentration, average size, polydispersity) of the product silica.

Using realistic MCVD process variables, the conditions for operation in the particle transport-limited and reaction-limited regimes were identified. Operation in the former regime results in high single-pass reactant conversion and product particle deposition, but a significant fraction (40%) of the product particles is lost with the gas outflow. Although operation in the latter regime results in lower single-pass conversion and deposition efficiencies, it has a potential for achievement of high process yields and deposition rate through recycling the effluent gases since almost all product particles are collected at the preform walls.

Aside from the reactant conversion rate and the process deposition efficiency, this model also provides information regarding the evolution of the particle concentration and size distribution. This information is useful for understanding dopant condensation and dissolution onto silica particles during manufacture of multicomponent optical waveguides.

Acknowledgment

The authors acknowledge stimulating discussions with P. Biswas during the course of this research. The Center for Aerosol Processes was established by a grant from the Ohio Board of Regents through the Research Challenge Program. This work was supported in part by NSF grant CBT–8707144.

Notation

b = constant
b_0 = constant, Eq. 19
b_2 = constant, Eq. 25
B_1 = particle diffusivity constant, $k_B T_e/(162\pi^2)^{1/3}\mu$
B_2 = slip correction constant for diffusion, $3.314\lambda(\pi/6)^{1/3}$
B_3 = coagulation constant (continuum), $2k_B T_e/3\mu$
B_4 = slip correction constant for coagulation, $1.257\lambda(4\pi/3)^{1/3}$
B_5 = coagulation constant (free molecule), $(3/4\pi)^{1/6}(6k_B T_e/\rho_p)^{1/2}$
c_p = heat capacity of O_2, J/g · K
C = $SiCl_4$ concentration, mol/cm^3
C_0 = inlet concentration of $SiCl_4$, mol/cm^3
d_p = particle diameter, cm
d_p^* = equivalent diameter of a SiO_2 molecule, cm
D = diffusion coefficient of particle, cm^2/s
$\mathcal{D}$ = diffusivity of $SiCl_4$ in O_2, cm^2/s
E = activation energy for oxidation of $SiCl_4$, J/mol
E_D = deposition efficiency
E_R = $SiCl_4$ conversion
g = gravitational acceleration, cm/s^2
Gr = Grashof number, $8R^3\rho^2 g(T_{max} - T_{min})/(\mu^2 T_e)$
k_B = Boltzmann's constant
k_g = heat conductivity of O_2, J/cm · s
k_0 = preexponential Arrhenius rate constant, s^{-1}
K = thermophoretic coefficient
Kn = Knudsen number, $2\lambda/d_p$
L_1, L_2 = axial distances in reaction zone
m = molecular weight of gas
M_q = qth moment of aerosol size distribution
n = particle size distribution function
N_{av} = Avogadro's number
P = number of radial points for finite-difference method
Q = total gas flow rate through preform tube, L/min
Pe_h = Peclet number for energy transfer, $2RU/\alpha$
Pe_m = Peclet number for $SiCl_4$ mass transfer, $2RU/\mathcal{D}$
Pr = Prandtl number, ν/α
r = radial distance, cm
R = preform tube radius, cm
Re = Reynolds number, $2RU/\nu$
R_G = gas constant
S = rate of formation of SiO_2 molecules by oxidation, cm^{-3} · s^{-1}
T = gas temperature, K
T_e = average temperature, 0.5 $(T_{max} + T_{min})$, K
T_{max} = maximum tube temperature (just above torch), K
T_{min} = minimum tube temperature (downstream of torch), K
T_0 = inlet gas temperature, K
T^* = dimensionless temperature drop, $T_{min}/(T_{max} - T_{min})$
U = average gas velocity, cm/s
$v, \bar{v}$ = particle volume, cm^3
v_g = geometric mean volume of SiO_2 particle, cm^3
v_1 = volume of a SiO_2 molecule, cm^3
W = polydispersity index
z = axial distance of preform tube, cm

Greek letters

α = thermal diffusivity of O_2, $k_g/\rho C_p$, cm^2/s
β = coagulation coefficient
ΔH = heat of reaction for $SiCl_4$ oxidation, J/mol
ζ = coagulation coefficient for second moment
λ = mean free path of gas, $\nu(\pi m/2k_B T_e)^{1/2}$, cm
μ = viscosity of gas stream, g/cm · s
ν = kinematic viscosity, cm^2/s
ξ = coagulation coefficient for zeroth moment
ρ = density of gas stream, g/cm^3
ρ_p = density of SiO_2 particle, g/cm^3
σ = standard deviation of log normal size distribution

Subscripts

C = continuum regime
FM = free-molecule regime
m = mixing cup average

Literature Cited

Bird, R. B., W. E. Stewart, and E. N. Lightfoot, *Transport Phenomena,* Wiley, New York (1960).
Bohrer, M. P., J. A. Amelse, P. L. Narasimham, B. K. Tariyal, J. M. Turnipseed, R. F. Gill, W. J. Moebuis, and J. L. Bodeker, "A Process for Recovering Germanium from Effluents of Optical Fiber Manufacturing," *J. Lightwave Technol.*, **LT-3,** 699 (1985).
Brock, J. R., and J. Oates, "Moment Simulation of Aerosol Evaporation," *J. Aerosol Sci.*, **18,** 59 (1987).
Carslaw, H. S., and J. C. Jaeger, *Conduction of Heat in Solids,* 2nd ed., Oxford, Great Britain, (1980).
Ferziger, J. H., *Numerical Methods for Engineering Applications,* Wiley, New York (1981).
French, W. G., L. J. Pace, and V. A. Foertmeyer, "Chemical Kinetics of the Reactions of $SiCl_4$, $SiBr_4$, $GeCl_4$, $POCl_3$ and BCl_3 with Oxygen," *J. Phys. Chem.*, **82,** 2191 (1978).
Friedlander, S. K., *Smoke, Dust and Haze,* Wiley, New York (1977).
Friedlander, S. K., and C. S. Wang, "The Self-Preserving Particle Size Distribution for Coagulation by Brownian Motion," *J. Colloid Interf. Sci.*, **22,** 126 (1966).
Fuchs, N. A., and A. G. Sutugin, *Topics in Current Aerosol Research,* G. M. Hidy, J. R. Brock, eds., Pergamon, Oxford, ch. 3 (1971).
Hinds, W. C., *Aerosol Technology,* Wiley, New York (1982).
IMSL, *IMSL Contents Document,* 8th ed., Int. Math. Statistical Libraries, Houston (1980).
Ingebrethsen, B. J., E. Matijevic, and R. E. Partch, "Preparation of Uniform Colloidal Dispersions by Chemical Reactions in Aerosols. III: Mixed Titania/Alumina Colloidal Spheres," *J. Colloid Interf. Sci.*, **95,** 228 (1983).
Kao, C. K., *Optical Fiber Systems: Technology, Design, and Application,* McGraw-Hill, New York (1982).
Kays, W. M., and H. C. Perkins, *Handbook of Heat Transfer,* 2nd ed., W. M. Rohsenow, J. P. Hartnett, E. N. Ganic, eds., McGraw-Hill, New York, ch. 7 (1985).
Kim, K.-S., "Optical Fiber Preform Fabrication by Modified Chemical Vapor Deposition," Ph.D. Thesis, Univ. Cincinnati, in preparation (1988).
Kleinert, P., D. Schmidt, J. Kirchhof, and A. Funke, "About Oxidation of $SiCl_4$ and $GeCl_4$ in Homogeneous Gaseous Phase," *Kristall und Technik,* **15,** 585 (1980).
Lee, K. W., "Change of Particle Size Distribution During Brownian Coagulation," *J. Colloid Interf. Sci.*, **92,** 315 (1983).
Lee, K. W., and H. Chen, "Coagulation Rate of Polydisperse Particles," *Aerosol Sci. Technol.*, **3,** 327 (1984).
Lee, K. W., and J. A. Gieseke, "Simplified Calculation of Aerosol Penetration through Channels and Tubes," *Atmos. Environ.*, **14,** 1089 (1980).
Lee, K. W., and B. Y. H. Liu, "On the Minimum Efficiency and the Most Penetrating Particle Size for Fibrous Filter," *J. Air Pollut. Control Assoc.*, **30,** 377 (1980).
Lee, K. W., H. Chen, and J. A. Gieseke, "Log-Normally Preserving Size Distribution for Brownian Coagulation in the Free-Molecule Regime," *Aerosol Sci. Technol.*, **3,** 53 (1984).
MacChesney, J. B., P. B. O'Connor, and H. M. Presby, "A New Technique for Preparation of Low-Loss and Graded Index Optical Fibers," *Proc. IEEE,* **62,** 1278 (1974).
Mehrotra, S., and M. K. Alam, "Particle Deposition in Fabrication of Optical Fibers by the MCVD Process," *Aerosols: Formation and Reactivity,* 2nd Int. Aerosol Conf., Berlin, 972 (1986).
Morse, T. F., and J. W. Cipolla, Jr., "Laser Modification of Thermophoretic Deposition," *J. Colloid Interf. Sci.*, **97,** 137 (1984).
Morse, T. F., C. Y. Wang, and J. W. Cipolla, Jr., "Laser-Induced Thermophoresis and Particulate Deposition Efficiency," *ASME J. Heat Transfer,* **107,** 155 (1985).
Morse, T. F., D. DiGiovanni, C. Y. Wang, and J. W. Cipolla, Jr., "Laser Enhancement of Thermophoretic Deposition Process," *J. Lightwave Technol.*, **4,** 151 (1986).
Nagel, S. R., J. B. MacChesney, and K. L. Walker, "An Overview of the

Modified Chemical Vapor Deposition (MCVD) Process and Performance," *IEEE J. Quantum Electron.*, **QE-18,** 459 (1982).

Okuyama, K., Y. Kousaka, N. Tohge, S. Yamamoto, J. J. Wu, R. C. Flagan, and J. H. Seinfeld, "Production of Ultrafine Metal Oxide Aerosol Particles by Thermal Decomposition of Metal Alkoxide Vapors," *AIChE J.*, **32,** 2010 (1986).

Partus, F. P., and M. A. Saifi, "Lightguide Preform Manufacture," *Western Electric Engineer,* **24,** 38 (1980).

Powers, D. R., "Kinetics of $SiCl_4$ Oxidation," *J. Am. Ceram. Soc.*, **61,** 295 (1978).

Pratsinis, S. E., "Simultaneous Aerosol Nucleation, Condensation, and Coagulation in Aerosol Reactors," *J. Colloid Interf. Sci.*, (1988).

Pratsinis, S. E., and K.-S. Kim, "Particle Coagulation, Diffusion, and Thermophoresis in Laminar Tube Flow," *J. Aerosol Sci.* (1988).

Pratsinis, S. E., T. T. Kodas, M. P. Dudukovic, and S. K. Friedlander, "Aerosol Reactor Design: Effect of Reactor Type and Process Parameters or Product Aerosol Characteristics," *Ind. Eng. Chem. Process Des. Dev.*, **25,** 634 (1986).

Sarkar, A., "Fabrication Techniques for High-Quality Optical Fibers," *Fibers and Integrated Optics,* **5,** 135 (1985).

Simpkins, P. G., S. Greenberg-Kosinski, and J. B. MacChesney, "Thermophoresis: The Mass Transfer Mechanism in Modified Chemical Vapor Deposition," *J. Appl. Phys.*, **50,** 5676 (1979).

Talbot, L., R. K. Cheng, R. W. Schefer, and D. R. Willis, "Thermophoresis of Particles in a Heated Boundary Layer," *J. Fluid Mech.*, **101,** 737 (1980).

Tsang, T. S., and J. R. Brock, "On Ostwald Ripening," *Aerosol Sci. Technol.*, **3,** 283 (1984).

Ulrich, G. D., "Theory of Particle Formation and Growth in Oxide Synthesis Flames," *Combust. Sci. Technol.*, **4,** 47 (1971).

Ulrich, G. D., and J. W. Riehl, "Aggregation and Growth of Submicron Oxide Particles in Flames," *J. Colloid Interf. Sci.*, **87,** 257 (1982).

Ulrich, G. D., and N. S. Subramanian, "Particle Growth in Flames. III: Coalescence as a Rate-Controlling Process," *Combust. Sci. Technol.*, **17,** 119 (1977).

Walker, K. L., G. M. Homsy, and F. T. Geyling, "Thermophoretic Deposition of Small Particles in Laminar Tube Flow," *J. Colloid Interf. Sci.*, **69,** 138 (1979).

Walker, K. L., F. T. Geyling, and S. R. Nagel, "Thermophoretic Deposition of Small Particles in the Modified Chemical Deposition (MCVD) Process," *J. Am. Ceram. Soc.*, **63,** 552 (1980).

Warren, D. R., and J. H. Seinfeld, "Simulation of Aerosol Size Distribution Evolution in Systems with Simultaneous Nucleation, Condensation, and Coagulation," *Aerosol Sci. Technol.*, **4,** 31 (1985).

Weinberg, M. C., "Thermophoretic Deposition in a Tube with a Variable Wall Temperature," *J. Colloid Interf. Sci.*, **87,** 579 (1982).

———, "Efficiency Improvement in Thermophoretic Deposition," *Commun. Am. Ceram. Soc.*, **C-30** (1983).

Wood, D. L., K. L. Walker, J. B. MacChesney, J. R. Simpson, and R. Csencsits, "Germanium Chemistry in the MCVD Process for Optical Fiber Fabrication," *J. Lightwave Technol.*, **LT-5,** 277 (1987).

Manuscript received Nov. 30, 1987, and revision received Feb. 9, 1988.